Redox-responsive Host-Guest Association Between g-Cyclodextrin and Mixed-Metal Keggin-Type Polyoxometalates

Sa Yao, Clément Falaise, Soumaya Khlifi, Nathalie Leclerc, Mohamed Haouas, David Landy, Emmanuel Cadot

Redox-responsive Host-Guest Association Between γ-Cyclodextrin and Mixed-Metal Keggin-Type Polyoxometalates

Sa Yao,[a] Clément Falaise,[a] Soumaya Khlifi,[a] Nathalie Leclerc,[a] Mohamed Haouas,[a] David Landy,[b] and Emmanuel Cadot*[a]*

[a] Institut Lavoisier de Versailles, UMR 8180 CNRS, UVSQ, Université Paris-Saclay, Versailles, France. E-mail : mohamed.haouas@uvsq.fr, emmanuel.cadot@uvsq.fr

[b] Unité de Chimie Environnementale et Interactions sur le Vivant (UCEIV, EA 4492), ULCO, Dunkerque, France.

ABSTRACT: The complexation of Keggin-type polyoxometalates (POMs) with γ-cyclodextrin (γ-CD) leads to supramolecular inclusion assemblies in aqueous solution driven by chaotropic effect. The strength of the interaction between γ-CD and oxidized or one-electron reduced POMs in a series of molybdenum and vanadium monosubstituted phospho- and silico-tungstates, $[XW_{11}MO_{40}]^{n-}$ Keggin-type anions where X = P or Si and M = $Mo^{V/VI}$ or $V^{IV/V}$, has been evaluated by isothermal titration calorimetry (ITC), NMR spectroscopy and cyclic voltammetry. Such a study reveals the host-guest binding constant $K_{1:1}$ increases strongly with the decrease of the global ionic charge of the POM unit. There is almost one magnitude order of variation in $K_{1:1}$ per charge unit, where $K_{1:1}$ falls down from about 10^5 to values close to zero as ionic charge varies from 3- to 6-. Such POMs with molybdenum and vanadium addenda offer the possibility of tuning the host-guest association strength by simple addition/removal of one electron to POMs, opening new avenue for the design of smart materials through redox stimuli.

INTRODUCTION

Polyoxometalates (POMs) represent a class of water soluble metal-oxo clusters built from group V and VI transition metals in their highest oxidation states, e.g. V^{V}, Mo^{VI}, and W^{VI}.[1] This class of polyanions exhibits a wide range of structures and chemical compositions which provide diverse properties and make them useful components in various fields including catalysis, medicine, energy, and materials science.[2–5] Among the numerous physicochemical properties of POMs, their ability to exchange reversibly electrons is probably the most intriguing and remarkable one, and utilization of POMs in redox processes is now generalized and commonly employed.[2,3,6] The archetypal Keggin type heteropolyanions exhibit spherical shape composed of twelve metal centers M (Mo^{VI} or W^{VI}) and one heteroatom X such as P^{V} or Si^{IV} in its central site, with a general chemical formula $XM_{12}O_{40}^{n-}$, abbreviated hereafter $[XM_{12}]^{n-}$.[7] Mixed-metal Keggin anions $[XW_{11}M]^{n-}$ can be easily prepared from addition of metal addenda (M = $Mo^{V/VI}$ or $V^{IV/V}$) on monolacunary heteropolyoxotungstates such as $[PW_{11}O_{39}]^{7-}$ or $[SiW_{11}O_{39}]^{8-}$. The oxidized and the one-electron reduced forms of mixed-metal polyanions are highly stable in solution contrary to reduced heteropolytungstates which are easily oxidized in air. Therefore, the global charge of the molybdenum and vanadium monosubstituted Keggin anions $[XW_{11}M]^{n-}$ can be controlled and modulated by playing with the nature of the heteroatom X or the nature and the redox state of the metal addenda M.

One of the most striking supramolecular properties of Keggin anions arises from their ability to form in aqueous solution step-wise inclusion complexes with the toroidal γ-cyclodextrin macrocycle (γ-CD) (Figure 1).[8–10] Such intriguing host-guest association based on this natural cyclic oligosaccharide is shown to be driven by the chaotropic effect. In brief, this effect consists in a water structure recovery process resulting from the desolvation of the interacting units, i.e. POM and cavitand.[11] Actually, such an effect has been shown to correspond to one of the main contributors involved within various phenomena such as the adsorption of POMs on micelles surface,[12] the aggregation with proteins,[13,14] the structuring supramolecular network[15] or hierarchical ionic recognition process.[16] The chaotropic character of Keggin POMs has been clearly demonstrated, while some of them have even been identified as superchaotrope entities according to the Hofmeister classification.[10,12,17] Indeed, it has recently been shown that strength of such supramolecular host-guest associations depends mainly on the charge density of the

POM.[10,11] Furthermore, ITC measurements revealed that processes driven by the chaotropic effect exhibit specific thermodynamic signatures, corresponding to enthalpy gain correlated to entropic penalty.[11] Some of these hybrid CD/Keggin composites have shown improved performances in catalysis[18] or adsorption,[19] for which cooperative effects should play crucial role. Therefore, deeper characterization of the interactions between γ-CD and mixed-metal Keggin POMs is needed for better understanding of the synergetic effect between the two components and further innovative development of advanced composite materials.

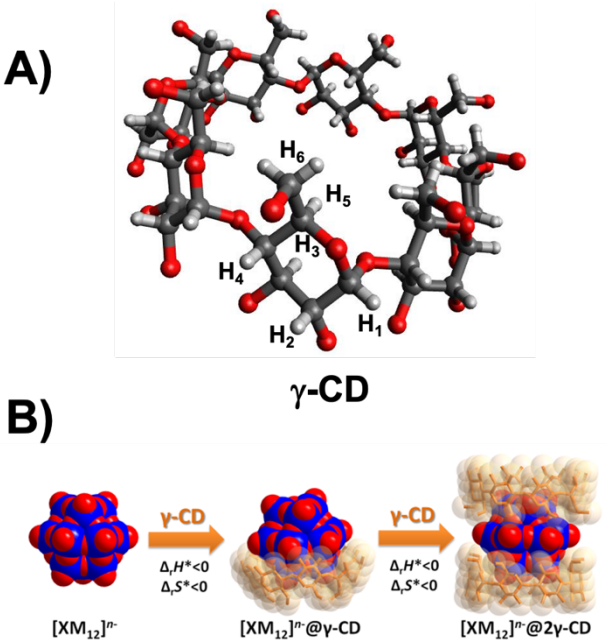

Figure 1. A) Structural representation of the macromolecular torus γ-CD ($C_{48}H_{80}O_{40}$) resulting from condensation of eight glucopyranose units. B) Step-wise complexation of Keggin anions $[XM_{12}]^{n-}$ and γ-CD resulting in 1:1 and 1:2 POM: γ-CD inclusion complexes $[XM_{12}]^{n-}$@γ-CD and $[XM_{12}]^{n-}$@2γ-CD. The process is enthalpically favorable but entropically unfavorable. The representations of supramolecular adducts shown correspond to crystallographic structures of $[PW_{12}]^{3-}$@γ-CD[9] and $[PMo_{12}]^{3-}$@2γ-CD.[8] Adapted from references 8 and 9 with permission from the Royal Society of Chemistry, and American Chemical Society.

In this contribution, we studied the interaction of γ-CD with mixed-metal Keggin anions $[XW_{11}MO_{40}]^{n-}$, where X = P^{V} or Si^{IV} and M = $Mo^{VI/V}$ or $V^{V/IV}$. Then, varying the redox state of

the Mo or the V atoms, complexation was observed in all cases as probed by nuclear magnetic resonance (NMR) spectroscopy, isothermal titration calorimetry (ITC), and cyclic voltammetry. However, binding affinity was found to depend mostly upon the global charge of the POM, rather than the nature of the addenda atom Mo or V. Actually, host-guest stability increases significantly with decreasing the global ionic charge of the Keggin POM in a similar way to previous report on Keggin-type polyoxotungstates $[XW_{12}]^{n-}$.[10] Thus, superchaotropic nature of low charged Keggin POMs was confirmed but can be easily canceled by simple one electron transfer within the POM unit. The current study represents basic fundamental knowledge for the development of smart supramolecular devices with responsive behavior based on change of the redox state of the POM unit.

EXPERIMENTAL SECTION

Syntheses of POMs. All reagents were purchased from commercial sources and used without further purification. Solutions were prepared in Milli-Q water. $Na_1K_3[PW_{11}V^{V}O_{40}]\bullet 7H_2O$ ($[PW_{11}V]^{4-}$),[20,21] $K_5[PW_{11}V^{IV}O_{40}]\bullet 14H_2O$ ($[PW_{11}V]^{5-}$),[22] $K_4[SiW_{11}Mo^{VI}O_{40}]\bullet 5H_2O$ ($[SiW_{11}Mo]^{4-}$),[23] $K_5[SiW_{11}Mo^{V}O_{40}]\bullet 12H_2O$ ($[SiW_{11}Mo]^{5-}$),[24] $K_5[SiW_{11}V^{V}O_{40}]\bullet 7H_2O$ ($[SiW_{11}V]^{5-}$),[20,25] and $Rb_5K_1[SiW_{11}V^{IV}O_{40}]\bullet 7H_2O$ ($[SiW_{11}V]^{6-}$),[21,26] were synthesized and purified according to published procedures. The molybdenum based phosphotungstates ($[PW_{11}Mo]^{3/4-}$) were also synthesized but they were found to be unstable in aqueous solution, and therefore they were not studied anymore. The purity and chemical composition of the POMs were confirmed by EDS, TGA, multinuclear NMR (^{29}Si, ^{31}P, ^{51}V, ^{95}Mo, and ^{183}W) and FT-IR spectroscopies. NMR and IR spectra are shown in Supporting Information (see Figures S1-7).

Characterizations of POMs. $Na_1K_3[PW_{11}V^{V}O_{40}]\bullet 7H_2O$. EDS: calc. W/V/P/K/Na: 11/1/1/3/1; obs. W/V/P/K/Na: 11/1.2/1.3/3.1/0.5. ^{31}P NMR, δ (ppm)/$\Delta\nu_{1/2}$ (Hz): -13.8/1. ^{51}V NMR, δ (ppm)/$\Delta\nu_{1/2}$ (Hz): -555.5/30. ^{183}W NMR, δ (ppm)/$\Delta\nu_{1/2}$ (Hz): -72.2/70, -98.5/1, -101.1/1, -103.5/1, -108.5/1, -108.6/50. FT-IR (cm^{-1}): 1099 (m), 1076 (m), 982 (s), 881 (m), 784 (s).

$K_5[PW_{11}V^{IV}O_{40}]\bullet 14H_2O$. EDS: calc. W/V/P/K: 11/1/1/5; obs. W/V/P/K: 11/1.1/1.5/5.4. ^{31}P NMR, δ (ppm)/$\Delta\nu_{1/2}$ (Hz): -4.1/1200. ^{183}W NMR, δ (ppm)/$\Delta\nu_{1/2}$ (Hz): -141.2/190, -169/200. FT-IR (cm^{-1}): 1088 (m), 1062 (m), 963 (s), 886 (m), 797 (s).

$K_4[SiW_{11}Mo^{VI}O_{40}]\cdot 5H_2O$. EDS: calc. W/Mo/Si/K: 11/1/1/4; obs. W/Mo/Si/K: 11/1.1/1/3.8. ^{29}Si NMR, δ (ppm)/$\Delta\nu_{1/2}$ (Hz): -84.1/0.4. ^{183}W NMR, δ (ppm)/$\Delta\nu_{1/2}$ (Hz): -100.8/1, -101.1/1, -103.2/1, -104.1/1, -104.3/1, -108.3/1. ^{95}Mo NMR, δ (ppm)/$\Delta\nu_{1/2}$ (Hz): 13.2/1100. FT-IR (cm^{-1}): 1016 (w), 973 (s), 920 (s), 877 (sh), 773 (s).

$K_5[SiW_{11}Mo^{V}O_{40}]\cdot 12H_2O$. EDS: calc. W/Mo/Si/K: 11/1/1/5; obs. W/Mo/Si/K: 11/0.9/0.3/4.9. ^{29}Si NMR, δ (ppm)/$\Delta\nu_{1/2}$ (Hz): -80.0/60. ^{183}W NMR, δ (ppm)/$\Delta\nu_{1/2}$ (Hz): -155/80, -201/160. FT-IR (cm^{-1}): 1009 (w), 966 (s), 913 (s), 860 (w), 770 (s).

$K_5[SiW_{11}V^{V}O_{40}]\cdot 7H_2O$. EDS: calc. W/V/Si/K: 11/1/1/5; obs. W/Mo/Si/K: 11/0.9/0.3/4.9. ^{29}Si NMR, δ (ppm)/$\Delta\nu_{1/2}$ (Hz): -84.5/0.5. ^{51}V NMR, δ (ppm)/$\Delta\nu_{1/2}$ (Hz): -549.1/40. ^{183}W NMR, δ (ppm)/$\Delta\nu_{1/2}$ (Hz): -78.4/70, -102.1/1, -112.1/1, -112.6/1, -118.7/1, -124.8/160. FT-IR (cm^{-1}): 1013 (w), 965 (s), 920 (vs), 880 (sh), 773 (s).

$Rb_5K_1[SiW_{11}V^{IV}O_{40}]\cdot 7H_2O$. EDS: calc. W/V/Si/K/Rb: 11/1/1/5/1; obs. W/Mo/Si/K: 11/0.9/1/5.3/0.7. ^{29}Si NMR, δ (ppm)/$\Delta\nu_{1/2}$ (Hz): -76.1/230. FT-IR (cm^{-1}): 1007 (w), 955 (s), 912 (vs), 798 (w), 698 (s).

Physical methods. Fourier transform infrared (FT-IR) spectra were recorded on a 6700 FT-IR Nicolet spectrophotometer, using the diamond ATR technique. The spectra were recorded on non-diluted compounds and ATR correction was applied. Energy-dispersive X-ray spectroscopy (EDS) measurements were performed using a SEM-FEG (scanning electron microscope enhanced by a field emission gun) equipment (JSM 7001-F, Jeol). The measures were acquired with a SDD XMax 50 mm^2 detector and the Aztec (Oxford) system working at 15 kV and 10 mm working distance. The quantification is realized with the standard library provided by the constructor using Lα lines. To determine water contents, thermal gravimetric analysis (TGA) measurements were performed using a Mettler Toledo TGA/DSC 1, STAR^e System apparatus under oxygen flow (50 mL min^{-1}) at a heating rate of 5 °C min^{-1} up to 700 °C.

Isothermal titration calorimetry (ITC). Formation constants and inclusion enthalpies were simultaneously determined for each γ-CD/POM system by the use of an isothermal calorimeter (ITC200, MicroCal Inc., USA). Degassed deionized water solutions were used in both cell (V_0 = 202.8 μL) and syringe (40 μL). After the addition of an initial aliquot of 1 μL, 10 aliquots of 3.5 μL of the syringe solution were delivered over 7 s for each injection. The time interval between two consecutive injections was 90 s, which proved to be sufficient for a systematic and

complete return to the baseline. The agitation speed was set to 1000 rpm. The resulting heat flow was recorded as a function of time. ITC titrations were realized at three temperatures (288, 298 and 308 K), with 5 mM γ-CD solution in the syringe and POM solution in the cell (0.25 mM for $[PW_{11}V]^{4-}$, 0.10 mM for $[SiW_{11}Mo]^{4-}$, 0.50 mM for $[SiW_{11}V]^{5-}$, $[PW_{11}V]^{5-}$, $[SiW_{11}Mo]^{5-}$, and $[SiW_{11}V]^{6-}$). Values and uncertainties of formation constants and inclusion enthalpies were determined by global analysis of the binding isotherms, by means of a dedicated homemade program, implementing 1:1 and 1:1 + 1:2 binding polynomials.

Cyclic Voltammetry (CV). Purified water was used throughout. It was obtained by passing water through a RiOs 8 unit followed by a Millipore-Q Academic purification set. All reagents were of high-purity grade and were used as purchased without further purification. CV experiments were carried out with an Methrohm Autolab PGSTAT12 potentiostat/galvanostat. Measurements were performed at room temperature in a conventional three-electrode cell. A glassy carbon (GC) electrode with a diameter of 3 mm was used as the working electrode. The auxiliary electrode was a Pt plate and potentials are quoted against Ag/AgCl electrode. The solutions were deaerated thoroughly for at least 10 minutes with pure argon and kept under a positive pressure of this gas during the experiments.

Nuclear magnetic resonance (NMR). All solution NMR spectra were measured in D_2O at 21 °C. ^{1}H, ^{29}Si, ^{31}P, ^{51}V, and ^{95}Mo NMR spectra were recorded on a Bruker Avance 400 spectrometer at Larmor frequencies of 400.1, 162.0, 105.2, 79.5, and 26.1 MHz, respectively, using 5 mm standard NMR tubes. The ^{183}W NMR spectra were obtained with 10 mm NMR tubes and a Bruker Avance 500 spectrometer operating at a Larmor frequency of 20.8 MHz. The ^{1}H NMR spectra were recorded with one pulse sequence at 30° flip angle (pulse duration 2.7 μs), using 0.1 s recycle delay, 3 s acquisition time, and 8 number of scans. Chemical shifts are scaled with respect to standards (δ = 0 ppm): Me_4Si (1% $CDCl_3$) for ^{1}H and ^{29}Si, H_3PO_4 for ^{31}P, $VOCl_3$ for ^{51}V, Na_2MoO_4 (D_2O, 2 M) for ^{95}Mo, Na_2WO_4 (D_2O, 1 M) for ^{183}W.

RESULTS AND DISCUSSION

To assess the strength of supramolecular interaction between the mixed-metal Keggin anions $[XW_{11}M]^{n-}$ and γ-CD, titration experiments were conducted in solution and the complexation was

monitored by three different techniques, namely cyclic voltammetry, NMR spectrometry, and isothermal titration calorimetry.

Cyclic voltammetry. POMs exhibit rich electrochemical behavior in solutions with redox response sensitive enough to their local environment (nature of the solvent, ion-pairing, protonation, etc.).[27] The interaction of $[XW_{11}M]^{n-}$ anions with γ-CD can be monitored through the variation of the half-wave potentials of the POM in presence of the tori host. A solution of 1 mM of the POM in acidic aqueous solution was then titrated with γ-CD varying its amount up to 50 equivalents. The resulting CVs obtained for the three oxidized forms of the mixed-metal Keggin anions $[PW_{11}V^{V}]^{4-}$, $[SiW_{11}Mo^{VI}]^{4-}$, and $[SiW_{11}V^{V}]^{5-}$ are shown in Figure 2. It should be mentioned that similar CV profiles were also obtained using the reduced forms $[PW_{11}V^{IV}]^{5-}$, $[SiW_{11}Mo^{V}]^{5-}$, and $[SiW_{11}V^{IV}]^{6-}$, shown in Supporting Information (see Figure S8).

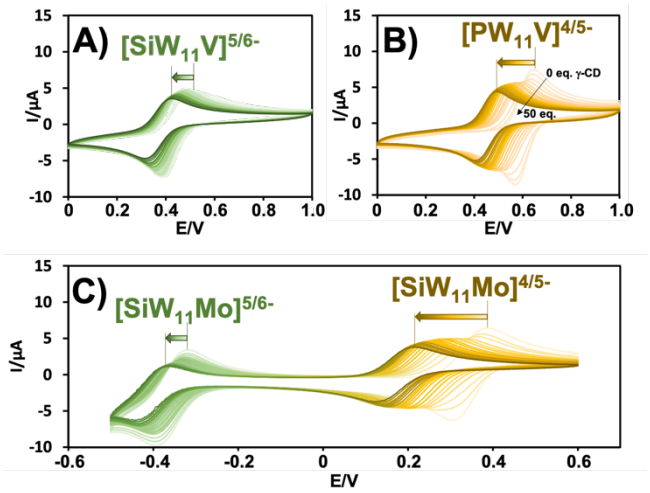

Figure 2. Cyclic voltammetry of the A) $[SiW_{11}V]^{5-}$, B) $[PW_{11}V]^{4-}$, and C) $[SiW_{11}Mo]^{4-}$ anions (1 $mmol.L^{-1}$, glassy carbon working electrode, Ag/AgCl reference electrode, scan rate 50 $mV.s^{-1}$) in the presence of increasing amounts of γ-CD (from 0 to 50 equivalents). The experiments have been performed in 50:50 (v:v) HCl (0.1 $mol.L^{-1}$):NaCl (0.9 $mol.L^{-1}$) aqueous solution for $[SiW_{11}V]^{5-}$ and $[PW_{11}V]^{4-}$, and 50:50 (v:v) H_2SO_4 (0.5 $mol.L^{-1}$):Na_2SO_4 (0.5 $mol.L^{-1}$) aqueous solution for $[SiW_{11}Mo]^{4-}$.

Presence of γ-CD leads to significant negative shifts of the half-wave potentials of the Keggin ion as an indication of host-guest complexes formation.[10] Effect of γ-CD has been

investigated on the first two quasi-reversible monoelectronic waves in the case of $[SiW_{11}Mo]^{4/5-}$ anions and only for the first exchange for V-derivatives because the second transfer in these POMs is not fully reversible and involve more than one electron. The negative shift in half-wave potentials indicates that the Keggin anions become more difficult to reduce in presence of γ-CD, meaning the γ-CDs interact much stronger with the oxidized species. Such an effect on redox properties of POMs is opposite to the ion-pairing effect observed in non-aqueous solvents with lithium or to the protonation in aqueous solution, which both result of stabilizing the reduced POM units.[28] Furthermore, the variation of the redox potential appears less pronounced as the ionic charge of the Keggin ion increases.[10] Then, as shown in Figure 3, the variation of the potential upon 50 equivalents addition of γ-CD appears larger for the redox couples $POM^{4-/5-}$ (about -150 mV for $[PW_{11}V]^{4/5-}$ and $[SiW_{11}Mo]^{4/5-}$) than for $POM^{5-/6-}$ couples (about -50 mV for $[SiW_{11}Mo]^{5/6-}$ and $[SiW_{11}V]^{5/6-}$). Such results reflect the influence of global charge density of the guest on the strength of the host-guest interaction. Concomitantly to the shift of the half-wave potentials, substantial decrease of the peak currents is also observed upon addition of supramolecular host. This is a direct evidence of the formation of inclusion complexes POM@*n*CD which diffuse with a slower rate in the aqueous electrolyte than γ-CD-free Keggin anions.

Variation of the observed half-wave potentials can be analyzed quantitatively to estimate the equilibrium constants ($K_{1:1}$ and $K_{1:2}$) of host-guest complexes formation involving the Keggin anions in its both oxidized and reduced states. Such an analysis considers the two consecutive steps of host-guest complexation given in equations (1) and (2) and the resulting Nernst equation (3).

$$[XW_{11}M]^{n-} + 2CD \overset{K_{1:1}^{ox}}{\longleftrightarrow} [XW_{11}M]^{n-}@CD + CD \overset{K_{1:2}^{ox}}{\longleftrightarrow} [XW_{11}M]^{n-}@2CD \quad (1)$$

$$[XW_{11}M]^{(n+1)-} + 2CD \overset{K_{1:1}^{red}}{\longleftrightarrow} [XW_{11}M]^{(n+1)-}@CD + CD \overset{K_{1:2}^{red}}{\longleftrightarrow} [XW_{11}M]^{(n+1)-}@2CD \quad (2)$$

$$E_{1/2} = E^0 + \frac{RT}{F} \ln \frac{(1+K_{1:1}^{ox}\,[CD]_{eq}+K_{1:1}^{ox}\,K_{1:2}^{ox}\,[CD]_{eq}^2)}{(1+K_{1:1}^{red}\,[CD]_{eq}+K_{1:1}^{red}\,K_{1:2}^{red}\,[CD]_{eq}^2)} \quad (3)$$

where E° is the standard redox potential of CD-free redox system $[XW_{11}M]^{n-}/[XW_{11}M]^{(n+1)-}$ and $[CD]_{eq}$ the concentration of solvated γ-CD in the equilibrium conditions. The binding

constants $K_{1:1}$ and $K_{1:2}$ are then obtained by fitting the experimental shift of the apparent potentials shown in Figure 3A-C. Analysis of the electrochemical data allows extracting general features that appear mainly directed by the global ionic charge of the involved species. Then, the redox behavior of the POM^{4-}/POM^{5-} couples is fairly modelled considering the three $K_{1:1}^{ox}$, $K_{1:2}^{ox}$ and $K_{1:1}^{red}$ stability constants associated to the consecutives processes written in equation (1) and (2) while the fourth $K_{1:2}^{red}$ stability constant can be neglected in the equation (3). Therefore, applying such a treatment for the $[PW_{11}V^{V}]^{4-}$ /$[PW_{11}V^{IV}]^{5-}$ and $[SiW_{11}Mo^{VI}]^{4-}/[SiW_{11}Mo^{V}]^{5-}$ systems gave satisfactory fits shown in Figure 3a-b, using stability constant values given in Table 2. Moreover, calculations of the redox behavior of the POM^{5-}/POM^{6-} system requires only the single $K_{1:1}^{ox}$ stability constant while the three others remain close to zero ($K_{1:2}^{ox} = K_{1:1}^{red} = K_{1:2}^{red} \approx 0$) and have been then neglected in the Nernst equation (3). In this way, the behavior of the second one-electron transfer involving the $[SiW_{11}Mo^{V}]^{5-}/[SiW_{10}W^{V}Mo^{V}]^{6-}$ system (see Figure 2C) has been modeled using $K_{1:2}^{ox} = 340\ M^{-1}$ while similar analysis for the $[SiW_{11}V^{V}]^{5-}/[SiW_{11}V^{IV}]^{6-}$ system leads to $K_{1:2}^{ox} = 590\ M^{-1}$ (see Figure 3D and Table 2). Thus, the behavior of the less charged ionic species POM^{4-} must be analyzed by taking into account the two consecutive complexation steps, while for the other anions POM^{5-} with larger ionic charge, only the 1:1 complex formation is significant. Furthermore, the $K_{1:1}$ stability constant exhibits the highest values (ca. 20000-9200) for the POM^{4-} anions and falls down of two orders of magnitude (ca. 600-300) as the ionic charge increases to give the POM^{5-} ion. At last, POM^{6-} species exhibit only negligible affinity for γ-CD as shown by corresponding $K_{1:1}$ and $K_{1:2}$ constant values close to zero. Furthermore, these calculated values determined by electrochemistry have been supported by other methods such as NMR or ITC, thus giving a set of coherent results that justifies the different data analyses carried out from complementary techniques (see Table 2).

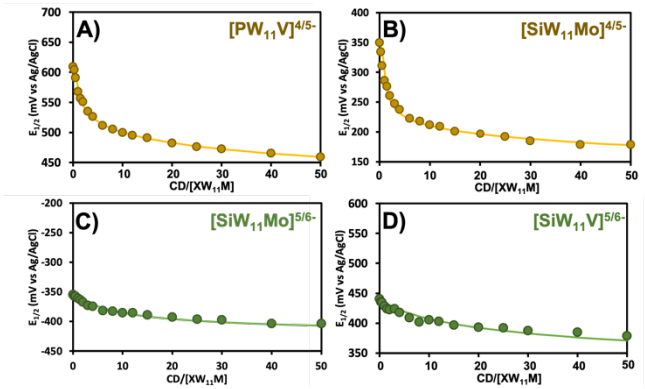

Figure 3. Variation of half-wave potential of the couple $[XW_{11}M]^{n/(n+1)-}$ observed in CVs of 1 mM A) $[PW_{11}V]^{4-}$, B) $[SiW_{11}Mo]^{4-}$, C) $[SiW_{11}Mo]^{5-}$, and D) $[SiW_{11}V]^{5-}$ as a function of molar ratio CD/$[XW_{11}M]$. The curves correspond to the best fit of experimental measurements (circles), calculated with equation (3).

^{1}H NMR spectroscopy. NMR is a popular technique to study cyclodextrins and their supramolecular complexes because such flexible macrocycles offer local NMR probes highly sensitive to through-space contact with guest molecules.[29] The formation and stability of mixed metal Keggin POM complexes with γ-CD were further investigated by ^{1}H NMR spectroscopy in D_2O. Here and in contrast to the electrochemistry study, we observe the supramolecular behavior from the state of the host in the presence of the guest. Therefore, an aqueous solution of 2 mM γ-CD is systematically titrated with the six different Keggin anions, respectively. The ^{1}H NMR spectra obtained in the range of 3.5 to 4.5 ppm corresponding to the protons of internal cavity are depicted in Figure 4, while the whole spectra are shown in the Supporting Information. Diamagnetic or paramagnetic nature of POM gives rise to different effects on the ^{1}H NMR spectrum profile through the supramolecular POM-CD interactions. Titrations with paramagnetic POMs $[PW_{11}V]^{5-}$, $[SiW_{11}Mo]^{5-}$, and $[SiW_{11}V]^{6-}$ induce gradual line broadening as a result of spin-electron dipolar interactions while interactions with diamagnetic POMs $[PW_{11}V]^{4-}$, $[SiW_{11}Mo]^{4-}$, and $[SiW_{11}V]^{5-}$leads to the typical chemical shift variations of the resonances attributed to involved hydrogen nuclei. Then, among the six γ-CD resonances, the H3, H5 and H6 resonances undergo significant alterations consistent with the partial inclusion of the Keggin anion within the γ-CD torus. However, the H6 signal exhibits the strongest effect observed as a low-field shift in the presence of diamagnetic POMs (see Figures 4A-C), or as a line-broadening in the presence of paramagnetic POMs (see Figures 4D-F). In both cases, these results should be consistent with

through-space host-guest contacts that involves the γ-CD primary rim in a labile complexation mode. As shown in Figures 4A and 4B, evolution of the ^{1}H NMR spectra upon titration is very similar for the $[PW_{11}VO_{40}]^{4-}$ and $[SiW_{11}MoO_{40}]^{4-}$ ions, indicating that the host-guest interaction is mostly directed by the global ionic charge rather than by the POM composition.[10] Furthermore, H6 resonance gives a single line in the presence of POM^{4-} ion (see Figures 4A and 4B), indicating a fast exchange process on the NMR time scale. Surprisingly, upon the $[SiW_{11}V]^{5-}$ addition, the shape of the H6 signal splits gradually from single line into two doublets (see Figure 4C). Such an evolution is related to a decrease of the dynamic involving the two H6 diastereotopic hydrogen nuclei and then suggests partial hindrance in the vicinity of the primary rim due to supramolecular POM^{5-}-CD interactions. Then, the H6 dynamics appear faster in the presence of the POM^{4-} ions, while the corresponding stability constants exhibit the highest values. Interestingly, similar features have been observed with the two Keggin-type polyoxotungstates $[SiW_{12}O_{40}]^{4-}$ and $[BW_{11}O_{40}]^{5-}$ ions showing that ionic charge dictates both the thermodynamic stability and the lability of the POM•••γ-CD supramolecular aggregates (see Figure S11).[10] Besides, these apparent contradictory results could be tentatively explained by considering the contributors within the ionic recognition process. In one hand, the solvent effects are predominant for low charge density species, identified as superchaotropes. Such a "pushing effect" leads to highly stable aggregates with γ-CD featured by very weak local attractive interactions (the "pulling effects" such as ion-dipole interactions or hydrogen bonding) consistent with labile associations. As the ionic charge increases, the chaopropic nature of the POM decreases and consecutively, the solvent effect (or the pushing effect) becomes less predominant leading to fragile aggregates but due to their higher ionic charge, the local "pulling effect" contributes to efficient ion-dipole interactions or hydrogen bonds involving the methanolic groups of the primary ring which become frozen on the NMR time scale. Such results and related explanations give evidences about the predominant role of the solvent within the aggregation process involving POM anions and non-ionic species such as γ-CD. In such systems, local attractive intermolecular forces have a minor influence within the thermodynamic stability which appears mainly governed by the chaotropic effect but have a major effect on the dynamics.

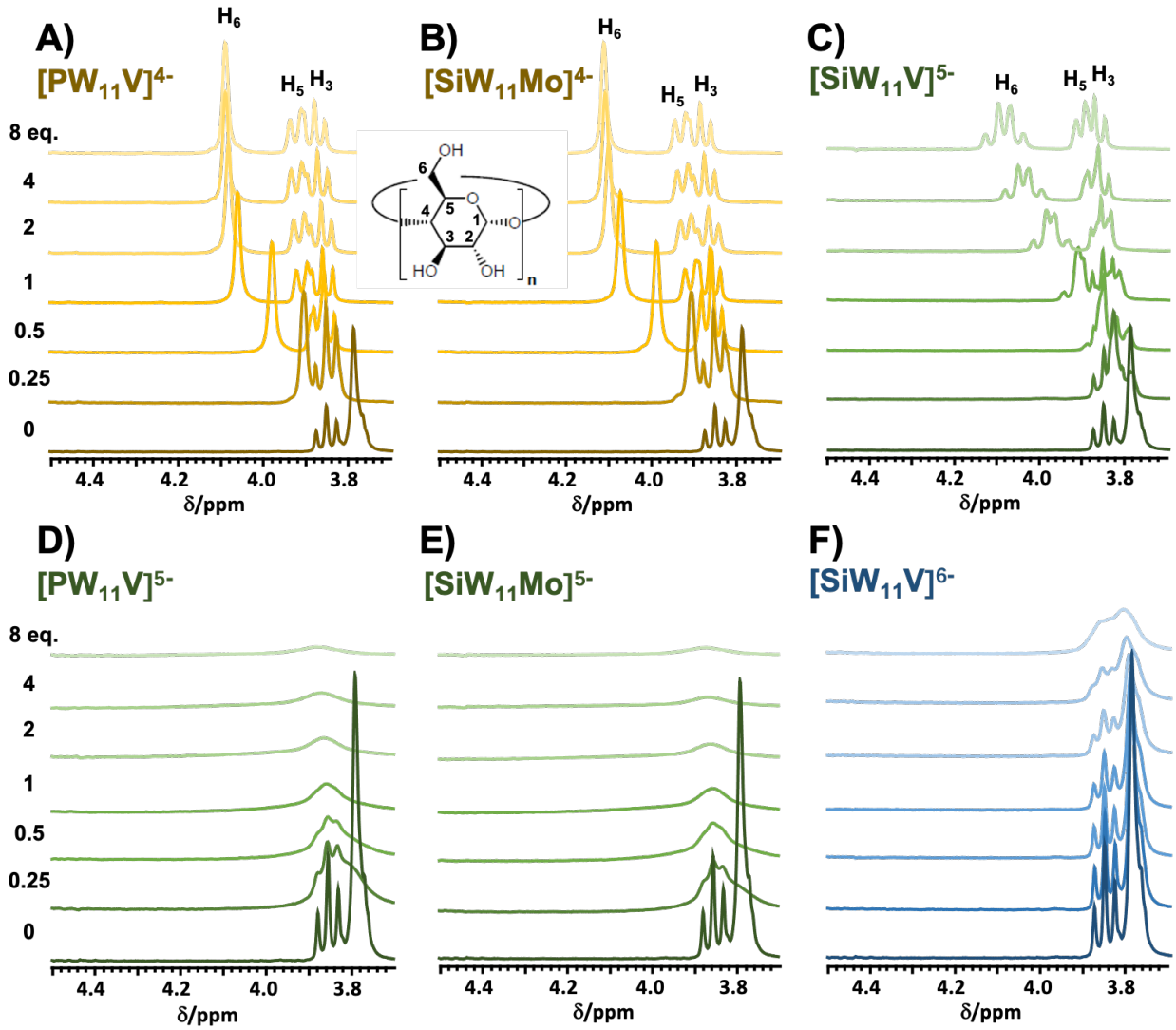

Figure 4. ^{1}H NMR spectra of γ-CD in the chemical shift range for H3, H5, and H6 protons resulting from the titration of 2 mM aqueous γ-CD solution with mixed metal Keggin anions A) $[PW_{11}V]^{4-}$, B) $[SiW_{11}Mo]^{4-}$, C) $[SiW_{11}V]^{5-}$, D) $[PW_{11}V]^{5-}$, E) $[SiW_{11}Mo]^{5-}$, and F) $[SiW_{11}V]^{6-}$.

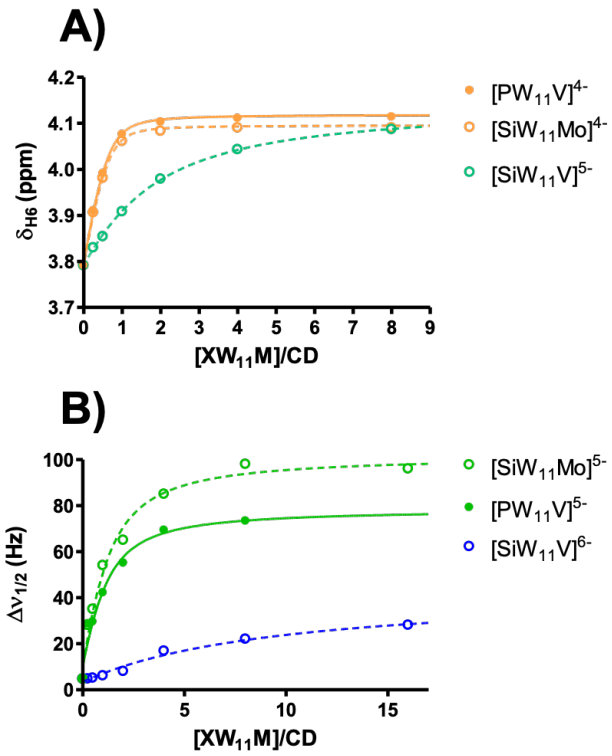

Figure 5. A) Chemical shifts for H6 and B) Average half-height line width $\Delta\nu_{1/2}$ of resonances H3, H5, and H6, as a function of the POM/CD molar ratio: the curves correspond to the best fit of experimental measurements (circles), calculated with equation (4).

The continuous variation of the NMR observables (noted Y) along titration (either chemical shift $Y = \delta$ or half-height line width $Y = \Delta\nu_{1/2}$) indicates the presence of CD-based aggregates in a global fast chemical exchange regime. The related observed values Y_{obs} should correspond to weighted average values of the three CD states, i.e. free CD and CD involved in 1:1 and 1:2 complexes represented by Y_0, $Y_{1:1}$ and $Y_{1:2}$ respectively. The apparent chemical shift $Y = \delta$ or half-height line width $Y = \Delta\nu_{1/2}$ could therefore be analyzed quantitatively using the following expression:

$$Y_{obs} = x_0\, Y_0 + x_{1:1}\, Y_{1:1} + x_{1:2}\, Y_{1:2} \qquad (4)$$

where x_0, $x_{1:1}$, $x_{1:2}$ are the γ-CD molar fractions corresponding respectively to its free state and in complexes with 1:1 and 1:2 stoichiometries. These molar fractions could be determined by combining the following relationships involving the binding constants $K_{1:1}$ and $K_{1:2}$ (see Supporting Information for more details):

$$K_{1:1} = \frac{x_{1:1}}{x_0\left(R-\left(\frac{1-x_0+x_{1:1}}{2}\right)\right)C^\circ} \quad (5), \qquad K_{1:2} = \frac{x_{1:2}}{2x_0x_{1:1}C^\circ} \quad (6), \text{ and } x_0 + x_{1:1} + x_{1:2} = 1 \quad (7)$$

Where C° corresponds to the initial concentration of γ-CD, and R = $[XW_{11}M]/[CD]$ is the introduced number of equivalents of POM. Finally, the observed NMR parameters Y_{obs} in eq. (4) depends on the constants $K_{1:1}$ and $K_{1:2}$, as well as Y_0, $Y_{1:1}$, and $Y_{1:2}$, and on the variable *R*. Figure 5 shows the calculated curves fitting the experimental data that allow extraction of the binding constants $K_{1:1}$ and $K_{1:2}$. The calculated values, summarized in Table 2, appear in fair agreement with those determined by electrochemistry, although the NMR values are systematically larger than those found by electrochemistry. Such differences should be attributed to the presence of electrolyte needed for the electrochemical measurements, which influences the ionic strength or could even compete to some extent within the POM-CD association process.

Although the moderate effect on line broadening observed in $[SiW_{11}V]^{6-}$ system can be modeled with a modest binding constant $K_{1:1}$ of 55 M^{-1} (Figure 5B), long-range paramagnetic effect could not be ruled out. To verify such a hypothesis similar NMR and CV titration experiments were carried out with α-CD and $[SiW_{11}V]^{6-}$. As expected, no inclusion could occur with this smaller host molecule since CV patterns were not altered at all with increasing amounts of POM (Figure S9). However, similar NMR line broadening effect to that observed with γ-CD was also noticed (Figure S12), which allows to conclude that the broadening in this case would be due to long range contact with paramagnetic POM species rather than to short range complexation. Thus, we could reasonably admit that no significant interaction would take place between this highly charged POM and γ-CD in agreement with previous electrochemical data and as it will be confirmed by ITC (see below).

Isothermal Titration Calorimetry. ITC experiments were carried out to provide detailed thermodynamic data about the recognition process of γ-CD with the six studied Keggin anions, respectively. ITC thermograms and isotherms are shown in Supporting Information section (see Figures S13 and S14), and thermodynamic parameters at 298 K Δ_rH^* and Δ_rS^* are given in Table 1 (for full data, see Table S2). Related stability constants at 298 K are provided in Table 2 for comparison with those determined by NMR and electrochemistry.

Table 1. Thermodynamic Parameters (kJ.mol^{-1}) at 298 K of 1:1 and 1:2 Complexation in Mixed Metal Keggin [$XW_{11}M$]:γ-CD Systems Measured by ITC.

[$XW_{11}M$]	[$XW_{11}M$]:CD	$\Delta_r H$*	$T\Delta_r S$*	$\Delta_r G$*
$[PW_{11}V]^{4-}$	1:1	-45.3 ± 0.7	-23.6 ± 0.8	-21.7 ± 0.1
	1:2	-39.7 ± 9.4	-26.3 ± 10.2	-13.4 ± 0.7
$[SiW_{11}Mo]^{4-}$	1:1	-40.2 ± 0.7	-16.8 ± 0.8	-23.4 ± 0.1
	1:2	-42.7 ± 4.4	-28.1 ± 4.8	-14.7 ± 0.3
$[SiW_{11}V]^{5-}$	1:1	-31.3 ± 1.6	-15.9 ± 1.6	-15.4 ± 0.1
	1:2	-[a]	-[a]	-[a]
$[PW_{11}V]^{5-}$	1:1	-39.9 ± 11.2	-27.7 ± 11.3	-12.2 ± 0.1
	1:2	-[a]	-[a]	-[a]
$[SiW_{11}Mo]^{5-}$	1:1	-34.0 ± 2.0	-19.3 ± 2.1	-14.8 ± 0.1
	1:2	-[a]	-[a]	-[a]
$[SiW_{11}V]^{6-}$	1:1	-[a]	-[a]	-[a]
	1:2	-[a]	-[a]	-[a]

[a] Negligeable heat detected.

Table 2. Binding Constants (M^{-1}) of γ-CD with the Keggin-Type POMs Measured by NMR, Electrochemistry, and ITC.

[$XW_{11}M$]	[$XW_{11}M$]:CD	NMR[b]	Electrochemistry[c]	ITC[d]
$[PW_{12}]^{3-a}$	1:1	140000	90000	
	1:2	800	1500	
$[SiW_{12}]^{4-}$	1:1	17000	9500	17200
	1:2	470	150	459
$[SiW_{11}Mo]^{4-}$	1:1	11000	20000	17700
	1:2	330	400	371
$[PW_{11}V]^{4-}$	1:1	7800	9200	8490
	1:2	320	220	222
$[PW_{12}]^{4-a}$	1:1		6000	
	1:2		30	
$[PW_{11}V]^{5-}$	1:1	860	290	164
	1:2	0	0	0
$[SiW_{11}Mo]^{5-}$	1:1	730	340	478
	1:2	0	0	0
$[SiW_{11}V]^{5-}$	1:1	390	590	618
	1:2	0	0	0
$[SiW_{12}]^{5-a}$	1:1		130	
	1:2		0	
$[SiW_{11}V]^{6-}$	1:1	0	0	0
	1:2		0	0
$[SiW_{11}Mo]^{6-}$	1:1		<30	
	1:2		0	

[a] From reference.[10] [b] Using chemical shift for diamagnetic POMs ($[PW_{12}]^{3-}$, $[SiW_{12}]^{4-}$, $[SiW_{11}Mo]^{4-}$, $[PW_{11}V]^{4-}$, and $[SiW_{11}V]^{5-}$) and half height line width for paramagnetic POMs ($[PW_{11}V]^{5-}$, $[SiW_{11}Mo]^{5-}$, and $[SiW_{11}V]^{6-}$). Accuracy below 30%. [c] Accuracy below 30%. [d] Accuracy below 8%.

As observed with previous chaotropic systems, host-guest supramolecular complexation of mixed Keggin anions with γ-CD is enthalpically driven counterbalanced by entropy penalty. The enthalpy changes range from ca. -30 to -40 kJ.mol^{-1} with POM^{5-} Keggin anions while they are slightly higher from ca. -40 to -45 kJ.mol^{-1} for complexation involving lower charged POMs $[XW_{11}M]^{4-}$. The entropy contribution varies however independently of the charge of the Keggin POM from ca. -15 to -30 kJ.mol^{-1} at 298 K. Consequently, complexes with less charged POMs $[XW_{11}M]^{4-}$ showed higher stability than those with higher charged POMs $[XW_{11}M]^{5-}$. This trend reflects nicely the results previously obtained by NMR and electrochemistry studies.

The ITC data were found consistent with the 1:2 binding model involving a sequential process for only $[PW_{11}V]^{4-}$ and $[SiW_{11}Mo]^{4-}$ POMs, whereas POM^{5-}-based systems ($[PW_{11}V]^{5-}$, $[SiW_{11}V]^{5-}$ and $[SiW_{11}Mo]^{5-}$) were analyzed considering only 1:1 stoichiometry. No significant heat exchange was observed in the case of the most charged $[SiW_{11}V]^{6-}$ ion consistent with negligible interactions with γ-CD. The overall results confirm the NMR and electrochemistry conclusions. ITC also revealed that the binding process is enthalpically driven, but accompanied by an entropic penalty as often observed in inclusion phenomenon with CD involving encapsulation of polynuclear chaotrope entities, such as dodecaborates or metal-atom clusters.[30,31] These thermochemical fingerprints are consistent with the chaotropic character of Keggin POMs.[10,11]

In summary, electrochemistry, NMR and ITC studies allowed to produce a convergent set of data, showing the close relationship between the supramolecular behavior of mixed metal Keggin-type derivatives toward γ-CD binding and the global ionic charge of the polyanion. These results are summarized in Figure 6, showing nicely that host-guest association strength is directly correlated with POM ionic charge. The $K_{1:1}$ stability constant for the first complexation step was found in the range of ca. 10^5 M^{-1} for the Keggin $[PW_{12}]^{3-}$ ion and drops down to ca. 10^4 M^{-1} for POM^{4-} ions and until ca. 10^2-10^3 M^{-1} for POM^{5-} species. Besides, the highest charged Keggin $[SiW_{11}V]^{6-}$ exhibited negligible values of $K_{1:1}$. Actually, such a variation corresponds to the decrease of the stability constant by one order of magnitude in average per increasing the global charge by one unit in similar way to previous study with Keggin anions $[XW_{12}]^{n-}$.[10] This follows nicely the classification of the chaotropic character of the Keggin POM previously established by its ability to adsorb on neutral micelle surfaces.[10,12] The current fundamental research shed light on the remarkable chaotropic behavior of POMs in solution and provide important basic

knowledge about supramolecular association involving POM species that could serve for rational design of advanced functional hybrid materials. Indeed, hybrid organic-inorganic hydrogels and polymers that exhibits changes in physical and chemical properties triggered by external stimuli is appealing functional materials with intricate features such as self-healing and shape-memory functions.[32] In context, unique behavior of CD-POM systems opens new perspectives for the design of redox-responsive smart materials.[33] For instance, the redox-active ferrocenyl group is frequently utilized in the fabrication of CD-based responsive supramolecular systems due to its ability to be encapsulated in or expelled from the β–CD cavity through a single-electron exchange process.[34,35] Keggin-type POMs, like ferrocene, are ideal molecular redox-switching units that possesses good size/shape matching with the larger macrocyclic receptor γ–CD. However, in the case of ionic species in aqueous medium, the driving forces are based mostly on the chaotropic character property rather than the hydrophobic effect. Thus, using hierarchical supramolecular recognition approach from preformed nano-objects constitutes a straightforward synthetic strategy to compartmentalize the complementary units embedded within hybrid supramolecular polymers, declined as coacervate, hydrogel, xerogel or aerogel derivatives.[36]

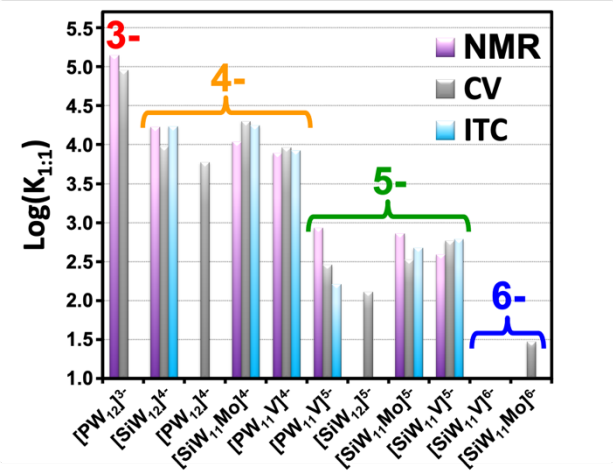

Figure 6. Order of magnitude of affinity constants of Keggin type POMs $[XM_{12}]^{n-}$ toward binding to γ-CD to form 1:1 supramolecular complex obtained from NMR, CV, and ITC, showing the general decreasing trend of association strength with increasing the global charge of the POM.

CONCLUSIONS

Driven by the chaotropic effect, the affinity between Keggin-type POMs and γ-CD can be tuned finely over a wide range of stability constants up to three order of magnitude of variation. It was shown that such a motif of assembly can be described as a "pushing effect" mainly orchestrated by the water molecules as solvent while we evidence by NMR that the "pulling factor", such as ion-dipole interaction or hydrogen bonding do not contribute significantly within the host-guest stability. Consistently, the global charge of the polyanion appears as the key factor affecting the strength of the host-guest association. Monosubstituted Keggin-type phospho- or silico-tungstates containing $Mo^{V/VI}$ or $V^{IV/V}$ as addenda offer a wide choice of redox active species $[XW_{11}M]^{n-}$ with standard potential in the [+ 0.6 ; -0.2] V. *vs* Ag/AgCl. Then, one-electron transfer is easily achievable and controllable either chemically or electrochemically resulting in significant change of the stability constants of the host-guest CD-POM complexes. This interesting property could be exploited in future application in the field of redox-responsive smart materials.

ASSOCIATED CONTENT

Supporting Information

The Supporting Information is available free of charge.

FT-IR and ^{29}Si, ^{31}P, ^{51}V, ^{95}Mo, and ^{183}W NMR spectra of Keggin POMs, additional ^{1}H NMR data, and ITC thermograms and isotherms.

AUTHOR INFORMATION

Corresponding Authors

* mohamed.haouas@uvsq.fr & emmanuel.cadot@uvsq.fr

ACKNOWLEDGMENTS

Authors gratefully acknowledge financial supports from LabEx CHARMMMAT (grant number ANR-11-LBX-0039), University of Versailles Saint-Quentin, and the CNRS (MOMENTUM grant). S.Y. thanks the China Scholarship Council (201904910419) for her scholarship.

DEDICATION

In memory of Francis Taulelle.

REFERENCES

(1) Gumerova, N. I.; Rompel, A. Polyoxometalates in Solution: Speciation under Spotlight. *Chem. Soc. Rev.* **2020**, *49* (21), 7568–7601. https://doi.org/10.1039/d0cs00392a.
(2) Sun, J.; Abednatanzi, S.; Van Der Voort, P.; Liu, Y.-Y.; Leus, K. POM@MOF Hybrids: Synthesis and Applications. *Catalysts* **2020**, *10* (5), 578. https://doi.org/10.3390/catal10050578.
(3) Huang, B.; Yang, D.-H.; Han, B.-H. Application of Polyoxometalate Derivatives in Rechargeable Batteries. *J. Mater. Chem. A* **2020**, *8* (9), 4593–4628. https://doi.org/10.1039/c9ta12679a.
(4) Colovic, M. B.; Lackovic, M.; Lalatovic, J.; Mougharbel, A. S.; Kortz, U.; Krsti, D. Z. Polyoxometalates in Biomedicine: Update and Overview. *Curr. Med. Chem.* **2020**, *27* (3), 362–379. https://doi.org/10.2174/0929867326666190827153532.
(5) Zhang, L.; Chen, Z. Polyoxometalates: Tailoring Metal Oxides in Molecular Dimension toward Energy Applications. *Int. J. Energy Res.* **2020**, *44* (5), 3316–3346. https://doi.org/10.1002/er.5124.
(6) Ma, P.; Hu, F.; Wang, J.; Niu, J. Carboxylate Covalently Modified Polyoxometalates: From Synthesis, Structural Diversity to Applications. *Coord. Chem. Rev.* **2019**, *378*, 281–309. https://doi.org/10.1016/j.ccr.2018.02.010.
(7) Keggin, J. F. The Structure and Formula of 12-Phosphotungstic Acid. *Proc. R. Soc. Lond. Ser. -Contain. Pap. Math. Phys. Character* **1934**, *144* (A851), 0075–0100. https://doi.org/10.1098/rspa.1934.0035.
(8) Wu, Y.; Shi, R.; Wu, Y.-L.; Holcroft, J. M.; Liu, Z.; Frasconi, M.; Wasielewski, M. R.; Li, H.; Stoddart, J. F. Complexation of Polyoxometalates with Cyclodextrins. *J. Am. Chem. Soc.* **2015**, *137* (12), 4111–4118. https://doi.org/10.1021/ja511713c.
(9) Jiang, Z.-G.; Mao, W.-T.; Huang, D.-P.; Wang, Y.; Wang, X.-J.; Zhan, C.-H. A Nonconventional Host-Guest Cubic Assembly Based on Gamma-Cyclodextrin and a Keggin-Type Polyoxometalate. *Nanoscale* **2020**, *12* (18), 10166–10171. https://doi.org/10.1039/d0nr00973c.
(10) Yao, S.; Falaise, C.; Ivanov, A. A.; Leclerc, N.; Hohenschutz, M.; Haouas, M.; Landy, D.; Shestopalov, M. A.; Bauduin, P.; Cadot, E. Hofmeister Effect in the Keggin-Type Polyoxotungstate Series. *Inorg. Chem. Front.* **2021**, *8* (1). https://doi.org/10.1039/d0qi00902d.
(11) Assaf, K. I.; Nau, W. M. The Chaotropic Effect as an Assembly Motif in Chemistry.

Angew. Chem.-Int. Ed. **2018**, *57* (43), 13968–13981. https://doi.org/10.1002/anie.201804597.
(12) Buchecker, T.; Schmid, P.; Grillo, I.; Prevost, S.; Drechsler, M.; Diat, O.; Pfitzner, A.; Bauduin, P. Self-Assembly of Short Chain PoIy-N-Isopropylacrylamid Induced by Superchaotropic Keggin Polyoxometalates: From Globules to Sheets. *J. Am. Chem. Soc.* **2019**, *141* (17), 6890–6899. https://doi.org/10.1021/jacs.8b12181.
(13) Sole-Daura, A.; Poblet, J. M.; Carbo, J. J. Structure-Activity Relationships for the Affinity of Chaotropic Polyoxometalate Anions towards Proteins. *Chem.- Eur. J.* **2020**, *26* (26), 5799–5809. https://doi.org/10.1002/chem.201905533.
(14) Paul, T. J.; Parac-Vogt, T. N.; Quinonero, D.; Prabhakar, R. Investigating Polyoxometalate-Protein Interactions at Chemically Distinct Binding Sites. *J. Phys. Chem. B* **2018**, *122* (29), 7219–7232. https://doi.org/10.1021/acs.jpcb.8b02931.
(15) Moussawi, M. A.; Leclerc-Laronze, N.; Floquet, S.; Abramov, P. A.; Sokolov, M. N.; Cordier, S.; Ponchel, A.; Monflier, E.; Bricout, H.; Landy, D.; Haouas, M.; Marrot, J.; Cadot, E. Polyoxometalate, Cationic Cluster, and Gamma-Cyclodextrin: From Primary Interactions to Supramolecular Hybrid Materials. *J. Am. Chem. Soc.* **2017**, *139* (36), 12793–12803. https://doi.org/10.1021/jacs.7b07317.
(16) Moussawi, M. A.; Haouas, M.; Floquet, S.; Shepard, W. E.; Abramov, P. A.; Sokolov, M. N.; Fedin, V. P.; Cordier, S.; Ponchel, A.; Monflier, E.; Marrot, J.; Cadot, E. Nonconventional Three-Component Hierarchical Host-Guest Assembly Based on Mo-Blue Ring-Shaped Giant Anion, Gamma-Cyclodextrin, and Dawson-Type Polyoxometalate. *J. Am. Chem. Soc.* **2017**, *139* (41), 14376–14379. https://doi.org/10.1021/jacs.7b08058.
(17) Buchecker, T.; Schmid, P.; Renaudineau, S.; Diat, O.; Proust, A.; Pfitzner, A.; Bauduin, P. Polyoxometalates in the Hofmeister Series. *Chem. Commun.* **2018**, *54* (15), 1833–1836. https://doi.org/10.1039/c7cc09113c.
(18) Ni, L.; Li, H.; Xu, H.; Shen, C.; Liu, R.; Xie, J.; Zhang, F.; Chen, C.; Zhao, H.; Zuo, T.; Diao, G. Self-Assembled Supramolecular Polyoxometalate Hybrid Architecture as a Multifunctional Oxidation Catalyst. *Acs Appl. Mater. Interfaces* **2019**, *11* (42), 38708–38718. https://doi.org/10.1021/acsami.9b12531.
(19) Yang, P.; Zhao, W.; Shkurenko, A.; Belmabkhout, Y.; Eddaoudi, M.; Dong, X.; Alshareef, H. N.; Khashab, N. M. Polyoxometalate-Cyclodextrin Metal-Organic Frameworks: From Tunable Structure to Customized Storage Functionality. *J. Am. Chem. Soc.* **2019**, *141* (5), 1847–1851. https://doi.org/10.1021/jacs.8b11998.
(20) Domaille, P. 1-Dimensional and Two-Dimensional W-183 and V-51 NMR Characterization of Isopolymetalates and Heteropolymetalates. *J. Am. Chem. Soc.* **1984**, *106* (25), 7677–7687. https://doi.org/10.1021/ja00337a004.
(21) Leparulo Loftus, M.; Pope, M. V-51 NMR-Spectroscopy of Tungstovanadate Polyanions - Chemical-Shift and Linewidth Patterns for the Identification of Stereoisomers. *Inorg. Chem.* **1987**, *26* (13), 2112–2120. https://doi.org/10.1021/ic00260a021.
(22) Rusu, D.; Baban, O.; Hauer, I.; Gligor, D.; David, L.; Rusu, M. Synthesis and Characterization of the Potassium 11-Tungstovanado(IV) Phosphate. *Rev. Roum. Chim.* **2010**, *55* (11–12), 843-+.
(23) Sanchez, C.; Livage, J.; Launay, J.; Fournier, M.; Jeannin, Y. Electron Delocalization in Mixed-Valence Molybdenum Polyanions. *J. Am. Chem. Soc.* **1982**, *104* (11), 3194–3202. https://doi.org/10.1021/ja00375a044.
(24) Li, C.; Sun, M.; Xu, L.; Wang, Y.; Huang, J. The First Heteropoly Blue-Embedded Metal-Organic Framework: Crystal Structure, Magnetic Property and Proton Conductivity.

Crystengcomm **2016**, *18* (4), 596–600. https://doi.org/10.1039/c5ce02074c.
(25) Bonfim, R. de P. F.; de Moura, L. C.; Pizzala, H.; Caldarelli, S.; Paul, S.; Eon, J. G.; Mentre, O.; Capron, M.; Delevoye, L.; Payen, E. Synthesis and Structural Characterization of a New Nanoporous-like Keggin Heteropolyanion Salt: K3(H2O)4[H2SiVW11O40](H2O)8+x. *Inorg. Chem.* **2007**, *46* (18), 7371–7377. https://doi.org/10.1021/ic700384m.
(26) Grigoriev, V. A.; Cheng, D.; Hill, C. L.; Weinstock, I. A. Role of Alkali Metal Cation Size in the Energy and Rate of Electron Transfer to Solvent-Separated 1 : 1 [(M+)(Acceptor)] (M+ = Li+, Na+, K+) Ion Pairs. *J. Am. Chem. Soc.* **2001**, *123* (22), 5292–5307. https://doi.org/10.1021/ja010074q.
(27) Sadakane, M.; Steckhan, E. Electrochemical Properties of Polyoxometalates as Electrocatalysts. *Chem. Rev.* **1998**, *98* (1), 219–237. https://doi.org/10.1021/cr960403a.
(28) Konishi, T.; Kodani, K.; Hasegawa, T.; Ogo, S.; Guo, S.-X.; Boas, J. F.; Zhang, J.; Bond, A. M.; Ueda, T. Impact of the Lithium Cation on the Voltammetry and Spectroscopy of [XVM11O40](n-) (X = P, As (N=4), S (N=3); M = Mo, W): Influence of Charge and Addenda and Hetero Atoms. *Inorg. Chem.* **2020**, *59* (15), 10522–10531. https://doi.org/10.1021/acs.inorgchem.0c00876.
(29) Schneider, H. J.; Hacket, F.; Rudiger, V.; Ikeda, H. NMR Studies of Cyclodextrins and Cyclodextrin Complexes. *Chem. Rev.* **1998**, *98* (5), 1755–1785. https://doi.org/10.1021/cr970019t.
(30) Assaf, K. I.; Ural, M. S.; Pan, F.; Georgiev, T.; Simova, S.; Rissanen, K.; Gabel, D.; Nau, W. M. Water Structure Recovery in Chaotropic Anion Recognition: High-Affinity Binding of Dodecaborate Clusters to -Cyclodextrin. *Angew. Chem.-Int. Ed.* **2015**, *54* (23), 6852–6856. https://doi.org/10.1002/anie.201412485.
(31) Ivanov, A. A.; Falaise, C.; Abramov, P. A.; Shestopalov, M. A.; Kirakci, K.; Lang, K.; Moussawi, M. A.; Sokolov, M. N.; Naumov, N. G.; Floquet, S.; Landy, D.; Haouas, M.; Brylev, K. A.; Mironov, Y. V.; Molard, Y.; Cordier, S.; Cadot, E. Host-Guest Binding Hierarchy within Redox- and Luminescence-Responsive Supramolecular Self-Assembly Based on Chalcogenide Clusters and Gamma-Cyclodextrin. *Chem.- Eur. J.* **2018**, *24* (51), 13467–13478. https://doi.org/10.1002/chem.201802102.
(32) Sinawang, G.; Osaki, M.; Takashima, Y.; Yamaguchi, H.; Harada, A. Supramolecular Self-Healing Materials from Non-Covalent Cross-Linking Host-Guest Interactions. *Chem. Commun.* **2020**, *56* (32), 4381–4395. https://doi.org/10.1039/d0cc00672f.
(33) Liu, X.; Zhao, L.; Liu, F.; Astruc, D.; Gu, H. Supramolecular Redox-Responsive Ferrocene Hydrogels and Microgels. *Coord. Chem. Rev.* **2020**, *419*, 213406. https://doi.org/10.1016/j.ccr.2020.213406.
(34) Aramoto, H.; Osaki, M.; Konishi, S.; Ueda, C.; Kobayashi, Y.; Takashima, Y.; Harada, A.; Yamaguchi, H. Redox-Responsive Supramolecular Polymeric Networks Having Double-Threaded Inclusion Complexes. *Chem. Sci.* **2020**, *11* (17), 4322–4331. https://doi.org/10.1039/c9sc05589d.
(35) Sinawang, G.; Osaki, M.; Takashima, Y.; Yamaguchi, H.; Harada, A. Biofunctional Hydrogels Based on Host-Guest Interactions. *Polym. J.* **2020**, *52* (8), 839–859. https://doi.org/10.1038/s41428-020-0352-7.
(36) Baroudi, I.; Sirnonnet-Jegat, C.; Roch-Marchal, C.; Leclerc-Laronze, N.; Livage, C.; Martineau, C.; Gervais, C.; Cadot, E.; Carn, F.; Fayolle, B.; Steunou, N. Supramolecular Assembly of Gelatin and Inorganic Polyanions: Fine-Tuning the Mechanical Properties of Nanocomposites by Varying Their Composition and Microstructure. *Chem. Mater.* **2015**, *27* (5),

1452–1464. https://doi.org/10.1021/cm502605q.

Table of Contents Synopsis

The complexation of polyoxometalates with γ-cyclodextrin leads to supramolecular inclusion assemblies in aqueous solution driven by chaotropic effect. Molybdenum and vanadium monosubstituted phospho- and silico-tungstate Keggin-type anions offer a convenient way to introduce and remove one electron in controllable manner, and thus to modulate the strength of the host guest association. Such a system would be promising for the design of smart materials based on redox stimuli.

Table of Contents Graphic